DOI 10.1515/pterid-2013-0023 — Pteridines 2013; 24(3-4): 191–199

Apsara Batra* and V. Girija Sastry

Extraction of ursolic acid from *Ocimum sanctum* and synthesis of its novel derivatives: effects on extracellular homocysteine, dihydrofolate reductase activity and proliferation of HepG2 human hepatoma cells

Abstract: The objective of the present study was to extract ursolic acid (UA) from *Ocimum sanctum*, to synthesize its bioactive derivatives, evaluate the anti-cancer effect of its derivatives and to establish the possible mechanism of action. In the present report, we extracted UA from whole plant of *O. sanctum*, synthesized its novel derivatives and investigated their effect on homocysteine metabolism and dihydrofolate reductase (DHFR) activity of HepG2 cells. UA and its derivatives UA-1, UA-2 and UA-3 down-regulated DHFR activity and increased extracellular homocysteine. UA-2 showed significant anti-proliferation activity in cancer cells. Cancer cells have increased the requirement of pyrimidine base thymidylate due to rapid cell division. Thymidylate biosynthesis depends on sufficient pools of folate dependent enzymes like DHFR. In the present study, we examined the UA and its derivatives mediated perturbation of DHFR activity and extracellular homocysteine in HepG2 human hepatoma cells. After incubation with UA-2, a potent inhibition of DHFR activity was observed. Our results showed that derivatization of UA might adversely affect DHFR activity. Measurement of extracellular homocysteine indicated impaired one-carbon metabolism in cells treated with UA derivatives. In conclusion, our data suggest an anti-cancer role of UA and its derivatives via inhibition of one-carbon metabolism.

Keywords: dihydrofolate reductase; HepG2; homocysteine; synthesis; ursolic acid.

***Corresponding author: Apsara Batra,** Pharmaceutical Chemistry Division, NCRD'S Sterling Institute of Pharmacy, Sector 19, Nerul (E), Nerul, Navi-Mumbai 400706, Maharashtra, India, E-mail: apsarabatra@gmail.com
V. Girija Sastry: Department of Pharmaceutical Chemistry, University College of Pharmaceutical Sciences, Andhra University, Visakhapatnam, Andhra Pradesh, India

Introduction

Ocimum sanctum (English: Holy Basil; Family: Labiatae) is a medicinal small herb and its many species have found extensive application in the indigenous system of medicine [1, 2]. Plants of *O. sanctum* are fragrant, aromatic and possess anti-catarrhal and expectorant properties [3]. Previous studies on *O. sanctum* have shown anti-cancer, hypotensive, cardiac depressant, smooth muscle cell relaxant and anti-stress activities [4, 5]. In addition, infusions of *O. sanctum* are used in traditional medicine to decrease plasma lipid content [6, 7]. Ursolic acid (UA) is the main active ingredient of *O. sanctum,* which is considered responsible for many of its therapeutic properties [8]. UA is a pentacyclic triterpene compound reported to possess a wide range of pharmacological properties, including anti-inflammatory, anti-allergic, antibacterial, antiviral and anti-tumor activities [9–13]. Among these interesting biological activities, the most intriguing property is the high cytotoxic activity. Renewed interest in the cytotoxic activity of triterpenes has come from the findings that betulinic acid exhibited selective cytotoxicity against melanoma and had apoptosis induction properties [14]. Considerable structural modification has been performed on betulinic acid and potentially important derivatives, which may be developed as anti-tumor drugs, have been produced. However, when compared to betulinic acid derivatives, UA derivatives have not been thoroughly explored for their cytotoxic activity. In order to find biologically more active derivatives of this naturally occurring triterpene, we selected *O. sanctum* extract as the source of UA.

Earlier studies have indicated that anti-cancer effect of UA involves inhibition of folate dependent one-carbon metabolism [15]. Folate-mediated one-carbon metabolism (FOCM) is a network of interrelated biochemical reactions that involve successive transfer of one-carbon

groups to a wide variety of biochemical molecules such as DNA, proteins and lipids [16, 17]. It also plays a central role in the remethylation of homocysteine (Hcy). Inhibition of FOCM involved in one-carbon flux toward thymidylate synthesis is associated with apoptosis of cancer cells [18]. Enzymes in the FOCM pathways such as dihydrofolate reductase (DHFR) are particular target of anticancer drugs [19]. DHFR (E.C. 1.5.1.3.), a key enzyme in thymidine synthesis, catalyzes the NADPH dependent reduction of dihydrofolate (DHF) to tetrahydrofolate (THF) [20, 21]. DHFR is ubiquitous and is of considerable pharmacological interest because of its key catalytic role in the formation of one-carbon donor THF. THF is an essential cofactor involved in the conversion of deoxyuridylate (dUMP) to deoxythymidylate (dTMP). Therefore, DHFR is a critical enzyme in DNA synthesis and has become a target for drug development and cancer therapy [22]. Hcy is a non-protein forming thiol containing amino acid formed by demethylation of methionine [23]. It is metabolized by remethylation to methionine or by trans-sulphuration to cysteine [24]. Present study was planned to extract UA from *O. sanctum*, synthesize its derivatives and to observe the effect of UA derivatives on cellular DHFR, extracellular Hcy and cell proliferation of HepG2 cells.

Based on the reports that the ester functionality at C-3 is essential for the pharmacological activities of pentacyclic triterpenes, and a hydrogen donor group at either C-3 position and/or C-28 position of UA is essential for the cytotoxic activity [25], UA derivatives (UA-1, UA-2 and UA-3) have been synthesized and their cytotoxic activities have been evaluated *in vitro* against cancer cell lines [26]. Our present studies show that derivatives of UA are potential candidate as anti-cancer molecules. This information is currently unavailable and is essential to develop potential strategies utilizing one-carbon metabolism for developing novel anti-cancer molecules from natural products.

Materials and methods

Reagents

Ocimum sanctum whole plant powder was purchased from Total herb solutions Pvt. Ltd., Mumbai. The OS powder size used was 0.50–1.00 mm. All solvents were purchased from Hi Media Ltd., Mumbai, India. Standard UA was purchased from Sigma Aldrich Chemical Company, USA. All the other reagents were purchased from reputed manufacturers and were of reagent grade.

Extraction and quantification of ursolic acid

The methanol crude extract obtained was suspended in $CHCl_3$: MeOH (9:1) and subjected to gradient column chromatography by hexane, ethyl acetate and methanol in increasing polarity. The fractions were collected and monitored on TLC and tested for the presence of UA. And those fractions, which consisted of UA, were combined together and the solvent was removed under vacuum. Evaporation of the combined fractions containing UA led to a white solid. The isolated UA was well characterized by melting point, U.V. and I.R. spectra as well as by comparing with an authentic sample in TLC and HPTLC. The amount of UA in the extract was calculated by TLC using optical densitometry, with known concentrations of the samples and of commercial UA. Different parameters affecting the extraction such as extraction time, solute to solvent ratio, extraction temperature were optimized and the final extraction experiment at the optimized conditions. The UA was quantified using Camag HPTLC apparatus with spotting device-linomat V Automatic Sample Spotter (Camag, Muttenz, Switzerland); Syringe-100 μL (Hamilton), HPTLC chamber-Glass twin trough chamber for 20×10 cm plates (Camag); Densitometer-TLC Scanner with wincats software (Camag); HPTLC plates-20×10 cm, pre-coated with silica gel 60, 0.2 mm layer thickness (Merck, Darmstadt, Germany). A stock solution of UA (90% pure, 72 μg/mL) was prepared by dissolving 2 mg of accurately weighed UA in methanol and diluting to 25 mL with methanol. Aliquots (1–8 mL) of stock solution were transferred to 10 mL volumetric flasks and diluted with methanol to obtain standard solutions containing 7.2, 14.4, 21.6, 28.8, 36, 43.2, 50.4, and 57.6 μg/mL UA, respectively. Ten microliters each of the standard solutions of UA (72–576 ng/spot) were applied and HPTLC was performed. After development, the plates were dried at room temperature in air, derivatized with Liebermann Burchard reagent and scanned at 530 nm in absorbance mode using the tungsten lamp. The peak areas were recorded. Calibration curve of UA was obtained by plotting peak areas versus applied concentrations of UA. Twenty microliters of suitably diluted sample was applied in triplicate on an HPTLC plate. The plate was developed and scanned as described above. The peak areas and absorption spectra were recorded, and the amount of UA was calculated using its calibration curve.

NMR spectra of ursolic acid (3β-hydroxy-urs-12-en-28-oic acid)

White powder, 1H-NMR (DMSO-d6); The H1 NMR spectrum of UA contained the signals for seven skeletal methyl groups of which five were singlets at δ 0.64 (3H, s, H-24), 0.67 (3H, s, H-26), 0.86 (3H, s, H-25), 0.90 (3H, s, H-23), 1.07 (3H, s, H-27) and two were doublets at δ 0.81 (3H, d, J=5.9 Hz, H-29) and 0.93 (3H, d, J=6.8 Hz, H-30). The signal for H-5 and H-9 appeared as singlet at δ 0.62 and 1.60, respectively. The signal for olefin proton and proton at position 3 appeared as doublet of doublets at δ 5.32 (1H, dd, J=13.7; 3.5 Hz; H-12) and 3.19 (1H, dd, J=5.2; 9.5 Hz, H-3). Multiplet signals were observed for each two protons at δ 1.54 (2H, m, H-16), 1.57 (2H, m, H-1), 1.55 (2H, m, H-22), 1.45 (2H, m, H-2), 1.29 (2H, m, H-21), 1.26 (2H, m, H-7) and 1.03 (2H, m, H-15). Doublet of doublets was also observed for two protons at position 11 with different coupling constants at δ 2.12 (2H, dd, J=13.7; 3.5 Hz, H-11). Further signals at δ 2.50 (1H, d; J=11.1 Hz, H-18), 1.53 (1H, m, H-20), 1.49 (1H, m, H-6a), 1.31 (1H, m, H-19), 1.30 (1H, m, H-6b) were observed in the spectrum.

Synthesis of ursolic acid derivatives

UA (3 β-hydroxy-urs-12-en-28-oic acid) was used as the lead compound and the structure modification was done as shown in Figure 1. The purity of the product was established by obtaining single spot on TLC plate.

Compound UA-1 (3β-acetoxy-urs-12-en-28-oic acid) was prepared by reaction of UA with acetic anhydride in THF in the presence of 4-dimethyl amino pyridine (DMAP), then reacted with chromium trioxide in acetic acid solution containing 5% acetic anhydride to obtain the compound (3β-acetoxy-urs-11-oxo-12-en-28-oic acid). In brief, a solution of UA (300 mg, 0.658 mmol) in THF (10 mL), pyridine (1 mL), acetic anhydride (1 mL) and a small amount of DMAP was stirred for 4 h at room temperature. When the reaction was complete, the solvent was concentrated in vacuo and the solids were dispersed in water, then acidified to pH 3–4 with HCl, filtered, washed with water to neutrality, and dried at room temperature to give white solid UA-1 (purity >80%).

To prepare UA-2, compound UA-1 was reacted with chromium trioxide in acetic acid solution containing 5% acetic anhydride to obtain an intermediate, which was treated with oxalyl chloride to yield a crude intermediate (3β-acetoxy-urs-11-oxo-12-en-28-acyl chloride), which was further condensed with appropriate amino compounds in the presence of triethylamine to give UA-2 [N-(3β-acetoxy-urs-11-oxo-12-en-28-acyl) aniline]. In brief, a mixture of UA-1 (50 mg, 0.1 mmol) with acetic anhydride (0.75 mL), acetic acid (14.25 mL) and CrO_3 (99.6 mg, 0.1 mmol) was stirred for 4–6 h at room temperature. It was followed by addition of water (20 mL) and CH_2Cl_2 (20 mL). Water layer was extracted twice with CH_2Cl_2 and combined organic phase was washed with saturated $NaHCO_3$, then washed with water to neutrality. Reaction mixture was then dried over Na_2SO_4, filtered, and concentrated in vacuo generating a light green oil, which was dissolved in CH_2Cl_2 (10 mL), oxalyl chloride (0.2 mmol) and the mixture stirred for 20 h. Reaction solvent and unreacted oxalyl chloride were eliminated by vacuum. Then the residue was dissolved in cyclonexane (5 mL). Acyl chloride was mixed with CH_2Cl_2 (5 mL) and Et3N to adjust the pH to 9–10. The solution was stirred for 5 min and amine (0.3 mmol) was added in at room temperature. TLC detected the reaction completion. The dichloromethane was eliminated by vacuum and the mixture was acidified with concentrated HCl to pH 3–4. A white solid was precipitated, filtered, the filter cake was washed to neutrality with water and dried to give a white solid (purity >80%). This white solid was reacted with aniline (0.3 mmol) using the general procedure to give UA-2 (28.1 mg, yield: 46%); m.p. 215–217°C; IR (KBr): The IR spectra showed the bands as 3384, 2927, 1708, 1668, 1620, 1599, 1534, 1503, 1453, 1373, 1250, 754, 693 cm^{-1}; 1H-NMR ($CDCl_3$): The H1 NMR spectra contained the signals for seven skeletal methyl groups of which five were singlets (δ 0.85, 0.90, 0.93, 0.95, 1.01) and two were doublets (δ 0.83, 0.89). H1 NMR spectrum also showed the presence of five aromatic protons at δ 7.10-7.45 (m, 5H, Ar-H). The signal for olefinic H^+ appears at δ 5.67 (s, 1H, H-12) and for proton at C-3 appears at δ 4.55 (m, 1H, H-3). Further signals at δ 5.75 (s, 1H, NH) and at δ 2.05 (S, 3 H, $COCH_3$) were observed in the spectra. MS m/z: 605.0 [M+18]+; Elemental analysis (%, found) C, 77.68 (77.64); H, 8.98 (9.09); N, 2.29 (2.38). This led to structure conformation of compound 2.

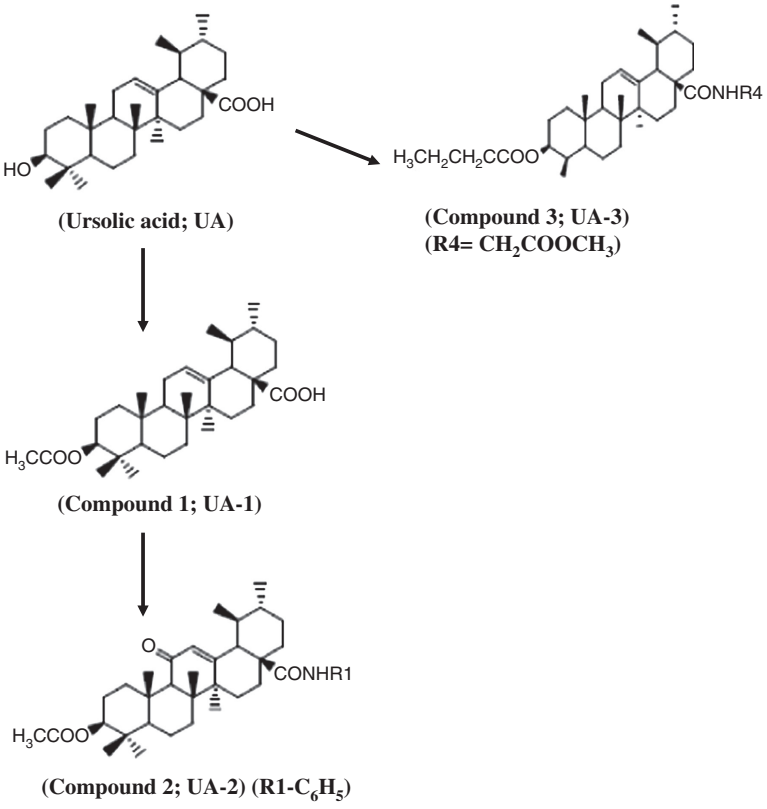

Figure 1 Synthesis of novel derivatives UA-1, UA-2 and UA-3 from ursolic acid. Reagents and conditions: (compound UA-1) Ac_2O, DMAP, THF, R.T; (compound UA-2) Ac_2O, DMAP, THF, R.T. followed by CrO_3, Ac_2O, AcOH, R.T. followed by CH_2Cl_2, $(COCl)_2$, R.T. followed by Et_3N, NH_2R1, R.T. (compound UA-3) $(CH_3CH_2CH_2)_2O$, DMAP, THF, R.T followed by CH_2Cl_2, $(COCl)_2$, R.T. followed by Et_3N, NH_2R4, R.T.

Compound UA-3 [Methyl N-(3β-butyryloxyl-urs-12-en-28-oyl)-2-amine acetate] was prepared by UA reacted with butyric anhydride in the presence of DMAP in THF. It was obtained from UA (100 mg, 0.22 mmol) and butyric anhydride by using the same method described for the preparation of derivative 1. Mixture in CH_2Cl_2 (2 mL) was stirred at room temperature for 20 h. The mixture was concentrated to dryness under reduced pressure. Cyclohexane (3×1 mL) was added to the residue, which was then concentrated to dryness to yield crude 3-*O*-butyryloxyl chloride. After addition of amine compound (0.44 mmol), the reaction mixture was stirred in the presence of Et3N (triethyl amine) at room temperature (TLC control). The resulting residue was partitioned in 3 mL water, then treated with 2 N HCl to pH 3, CH_2Cl_2 was removed under vacuum to precipitate white solid (purity >80%) that was filtered and the filter cake was washed with water to pH 7, and dried. Yield: 69.5%; m.p. 79–84°C; IR (KBr): 3384, 2895, 1720, 1659, 1531, 1465, 1305, 1023 cm^{-1}; The H1 NMR ($CDCl_3$) spectra contained the signals for methyl groups at δ 0.940 (s, 9H, CH_3×3), 0.850 (m, 12H, CH_3×4), 0.703 (s, 3H, CH_3) and 1.089 (s, 3H, CH_3). The signal for olefinic H^+ appears at δ 5.395 (t-like, 1H, H-12), a broad singlet was observed at δ 4.075–4.115 (br, 1H, NHCHa), 3.809–3.846 (br, 1H, NHCHb). The spectrum revealed the multiplet at δ 6.515 (m, 1H, NH), and for proton at C-3 appears at δ 4.485 (m, 1H, H-3). Further signals at δ 3.749 (s, 3H, O CH_3), 2.273 (s, 3H, CH_3CO) were observed in the spectra. ESI-MS m/z: 598.6 (M+H)+; Elemental analysis (%, found) C, 73.96 (74.08); H, 10.15 (10.25); N, 2.45 (2.33). The target compounds were purified on a silica gel column with petroleum ether/ethyl acetate (or acetone) as eluents and their structures confirmed by mp, IR and elemental analysis. This led to structure conformation of compounds.

Study design

Human HepG2 cells were cultured in Dulbecco's modified eagles medium (DMEM) supplemented with 10% fetal calf serum (Sigma). Cells were maintained at 37°C in humidified atmosphere with 5% CO_2. For various biochemical assays, samples were divided into four groups as follows: 1) Groups 1, 2 and 3; sham controls: cells incubated with 0.05% DMSO for 24, 48 and 72 h; 2) Groups 4, 5 and 6; methotrexate control: cells exposed to 10^{-5} mol/L methotrexate for 24, 48 and 72 h; 3) Groups 7, 8 and 9; UA (UA): cells exposed to 10^{-5} mol/L UA for 24, 48 and 72 h; 4) Groups 10, 11 and 12; compound UA-1: cells exposed to 10^{-5} mol/L UA-1 for 24, 48 and 72 h; 5) Groups 13, 14 and 15; compound UA-2: cells exposed to 10^{-5} mol/L UA-2 for 24, 48 and 72 h; 6) Groups 16, 17 and 18; compound UA-3: cells exposed to 10^{-5} mol/L UA-3 for 24, 48 and 72 h.

For all experiments methotrexate, UA, UA-1, UA-2 and UA-3 were dissolved in DMSO. For sham control DMSO was diluted in medium to a concentration corresponding to the 0.05% DMSO in drug-treated groups.

Cell proliferation assay

Anti-proliferation activity of synthesized derivatives was evaluated *in vitro* using the WST-8 method against Hep G2 cells with UA as the positive control. Cells were incubated in 96-well plates ($5×10^3$ cells/well) and were allowed to attach for 24 h. After 24 h, the UA derivatives were added with different indicated concentrations of 10^{-5}, 10^{-6}, 10^{-7}, and 10^{-8} mol/L, respectively, for another 24, 48 and 72 h incubation. Number of viable cells was measured using a WST-8 assay. In brief, 10 µL WST-8 solution was added into each well and the cells were incubated for another 1 h. The absorbance of formazan formed in the untreated cells was considered as 100% and was measured at 450 nm. Absorbance ratio was calculated by dividing absorbance of the sample to that of the control. Percentage cell survival was calculated by multiplying absorbance ratio with 100.

Total homocysteine (t-Hcy) assay

Total homcysteine (t-Hcy) estimation involved cleavage and release of protein bound Hcy by DTT. Sadenosylhomocysteinase (SAHase) and excess adenosine (Ado) were used to convert free homocysteine (f-Hcy) and protein-released Hcy to S-adenosylhomocysteine (SAH). SAH levels were estimated by competitive immunoassay with an anti-SAH antibody. Due to the reversible nature of the SAHase reaction, thimerosal, an inhibitor of SAHase, was included to prevent hydrolysis of SAH back to Hcy. In brief, 25 µL of the SAHase-treated samples or calibrators were transferred to coated micro-titer wells. Two hundred microliters of anti-SAH antibody (67 µg/L in assay buffer 2) was added to each well, and the samples were incubated at ambient temperature (18–25°C) for 30 min. The micro-titer plate was washed three times, each time with 400 µL of washing solution per well, after which 200 µL of HRP-conjugated antibody (1.3 mg/L in stabilization buffer) was added to each sample. This plate was then incubated at ambient temperature for 30 min and then washed three times with 400 µL of washing solution per well. After addition of 200 µL of the HRP substrate to each well, the plate was incubated at ambient temperature for 10 min. The HRP reaction was stopped by adding 100 µL of 0.8 mol/L sulfuric acid per well, and the yellow color produced was measured at 450 nm.

Dihydrofolate reductase (DHFR) activity assay

DHFR (EC 1.5.1.3) was assayed essentially according to the method described earlier [27]. DHFR assay system contained, in a total volume of 1 mL, 100 mM DHF, 50 mM NADPH, 50 mM 2-mercaptoethanol and 5 µg enzyme protein in 50 mM Tris-HCl buffer (pH 7.4) containing 1 mM EDTA and 20 mM 2-mercaptoethanol. Enzymatic reactions were carried out at 30°C using appropriate blanks and the decrease in absorbance at 340 nm was monitored in a recording double beam Jasco V530 UV/VIS spectrophotometer. The readings were recorded in the initial 2 min linear phase of the reaction. Decrease in the absorbance at 340 nm was thus taken as a measure of THF produced enzymatically from DHF. The molar extinction coefficient at 340 nm for this reaction is approximately 12×103 cm^2/mol. One international unit of DHFR activity is defined as equivalent to the amount of enzyme required to transform 1 mol of DHFA to THFA per minute under condition of assay. All the chemicals and biochemicals used for DHFR assay were of analytical reagent grade. l-7,8-DHF, nicotinamide adenine dinucleotide phosphate, reduced form (NADPH), 2-mercaptoethanol and ethylenediaminetetraacetic acid (EDTA) were procured from Sigma-Aldrich Co., St. Louis, MO, USA.

Statistical analysis

All values were expressed as mean±standard error of means of samples with n and p indicated in the Results section. Statistical analyses were performed using Student's t-test (GraphPad QuickCalcs, San Diego, CA, USA). Values with $p<0.05$ were considered statistically significant.

Results

Various derivatives of ursolic acid (UA-1, UA-2 and UA-3) showed significant anti-proliferation activity against HepG2 human hepatoma cancer cells

Cells incubated with UA (10^{-8}, 10^{-7}, 10^{-6} and 10^{-5} mol/L) showed significant dose dependent decrease in cell viability. Cell viability decreased to 76% (approx.) after 72 h of incubation with 10^{-7} UA. A further increase in UA concentration from 10^{-7} mol/L to 10^{-5} mol/L could not significantly reduce cell viability. Exposure of HepG2 cells to various UA derivatives caused gradual decrease in percentage cell survival (Figure 2). Compound UA-2 [N-(3β-acetoxy-urs-11-oxo-12-en-28- acyl) aniline], showed significant toxicity after 24 h of exposure. Moreover, after 48 h of exposure significant loss of cell viability was observed. Exposing the HepG2 cells to 10^{-8}, 10^{-7}, 10^{-6} and 10^{-5} mol/L of UA-2 caused 78.3%, 44.5% and 37.3% cell survival after 24 h of incubation. Treatment of human hepatoma cells with 10^{-5} mol/L of various derivatives of UA showed most significant anti-proliferation effect. Therefore, various derivatives at concentration of 10^{-5} mol/L were chosen for assessing extracellular Hcy and DHFR activity.

Incubation of HepG2 cells with ursolic acid derivatives (UA-1, UA-2 and UA-3) increased extracellular homocysteine levels

Table 1 shows the extracellular Hcy profile of HepG2 cells after 24, 48 and 72 h of incubation. In control experiments, no significant change in Hcy levels was seen up to 72 h of incubation. Present studies showed no significant change in extracellular Hcy even after incubation with UA for 72 h ($p>0.005$). After 24 h of incubation with UA-1, Hcy

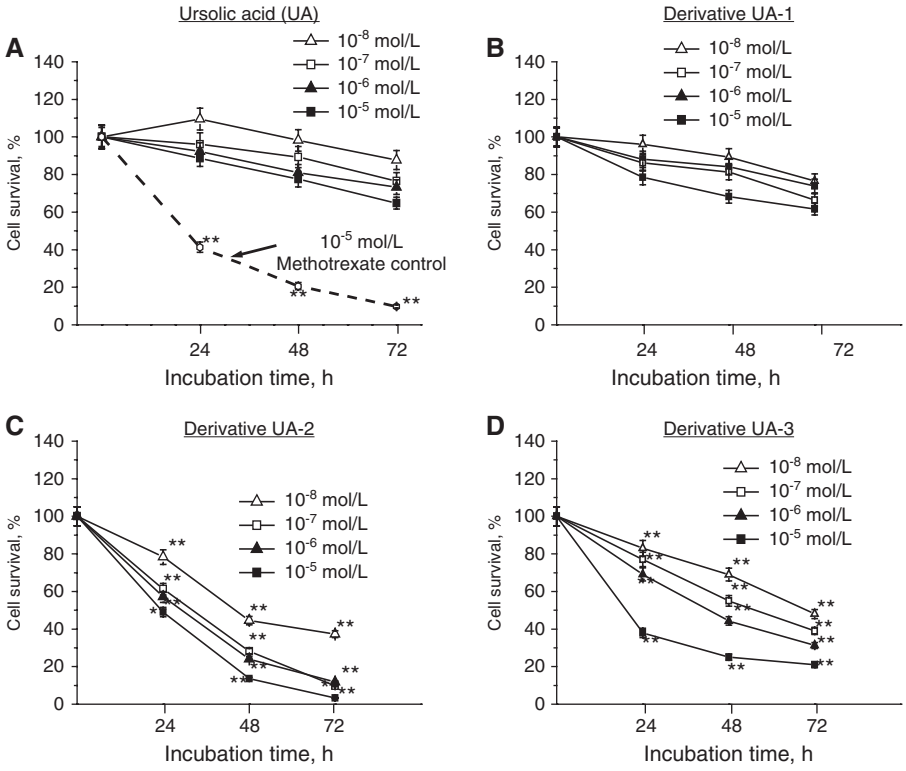

Figure 2 Effect of various doses of ursolic acid and its derivatives on time-dependent (0–72 h) survival of HepG2 human hepatoma cells using methotrexate as control. All values are mean±standard error of samples (in triplicate) from four different experiments in each group. (**$p<0.01$: indicate significance of difference between ursolic acid derivative treatment compared to ursolic acid treatment).

Table 1 Effect of ursolic acid and its novel synthesized derivatives UA-1, UA-2 and UA-3 on extracellular homocysteine concentration in HepG2 cells after 24, 48 and 72 h of incubation.

Treatment	Extracellular homocysteine concentration		
	24 h	48 h	72 h
Sham control	6.5±0.7	6.9±0.8	7.2±0.8
Methotrexate control	16.1±1.9[b]	24.8±2.7[b]	31.6±3.3[b]
Ursolic acid	7.1±0.7	7.3±0.7	7.6±0.8
Derivative UA-1	8.2±0.41[a]	9.0±0.9[a]	11.2±1.2[b]
Derivative UA-2	13.5±1.5[b]	17.7±1.9[b]	23.5±2.3[b]
Derivative UA-3	7.6±0.8	9.1±0.8[a]	9.7±0.9[a]

Extracellular homocysteine concentrations are expressed as nmol/mL medium. All values are mean±standard error of samples (in triplicate) from four different experiments in each group. ([a]$p<0.05$, [b]$p<0.01$: indicate significance of difference between ursolic acid or its derivatives treatment and control treatment groups.)

levels increased to 8.2±0.41 nmol/mL medium ($p<0.005$) compared to sham control (6.5±0.7). Hcy levels further increased to 9.0±0.9 and 11.2±1.2 after 48 and 72 h of incubation with UA-1. HepG2 cells exposed to UA-2, unlike those exposed to UA-1, showed extensive increase in the Hcy levels. Hcy levels rose up to 13.5±1.5, 17.7±1.9 and 23.5±2.3 after 24, 48 and 72 h of incubation, respectively. However, after incubation with UA-3, increase in Hcy level was less pronounced compared to UA-2. No significant changes in Hcy levels were observed after 24 h incubation with derivative 3. However, levels rose up to 9.1±0.8 and 9.7±0.9 after 48 and 72 h of incubation. These data indicated that derivatization of UA substituted at C-3 and C-28 with 11-oxo could significantly alter one-carbon metabolism of HepG2 cells and extracellular Hcy profile might be a marker of bioactivity of UA and its derivatives.

Incubation of HepG2 cells with derivatives of ursolic acid (UA-1, UA-2 and UA-3) inhibited cellular dihydrofolate reductase activity

To determine possible mechanisms leading to alterations in one-carbon metabolism in cancer cells, we analyzed the DHFR activity in HepG2 cells. DHFR was monitored in HepG2 cells after incubation with various derivatives of UA. No significant change in DHFR activity was seen in sham control experiments (Table 2). Significant decrease in DHFR activity was seen after 72 h of incubation with UA. The enzyme activity started decreasing steeply when cells were exposed for 72 h with acetyl derivative of UA (UA-1) (Table 2) where enzyme levels were 19.6±1.6 (control: 27.5±2.3). As shown in Table 2, cells incubated with UA-2 [N-(3β-acetoxy-urs-11-oxo-12-en-28- acyl) aniline], showed most significant decrease ($p<0.01$) in the enzyme activity. DHFR activity decreased to 9.4±1.1 after 72 h of incubation with UA-2. These results showed that incubation of HepG2 cells with UA derivatives substituted at C-3 and C-28 with 11-oxo might reduce DHFR enzyme more promptly, which in turn could alter one-carbon metabolism and extracellular Hcy levels. No statistically significant difference in DHFR activity was noticed when HepG2 cells were exposed for 24 h with UA-3 [Methyl N-(3β-butyryloxyl-urs-12-en-28-oyl)-2-amine acetate]. However, after 48 and 72 h of incubation enzyme activity decreased to 21.5±2.1 and 17.5±1.4, respectively.

Discussion

Many people around the world, for their day-to-day medicinal needs, rely on traditional medicine, which has been around for centuries [28]. Even modern medicine in most instances relies on natural products, and two-thirds of anti-cancer drugs have their roots in products derived from nature [29, 30]. Compounds from natural sources have an advantage in that they are usually multitargeted [31, 32]. One such compound is UA, a pentacyclic triterpenoid that has been identified in medicinal herb *O. sanctum* [33]. It has been shown that UA can inhibit cell proliferation and induce apoptosis in various tumors [34]. UA induces apoptosis through multiple pathways, such as inhibiting DNA replication [35, 36]. However, many investigators have proposed that anti-cancer activity of UA might be enhanced by derivatization while retaining ester functionality at C-3 and hydrogen donor group at either C-3 position and/or

Table 2 Effect of ursolic acid and its novel synthesized derivatives UA-1, UA-2 and UA-3 on cellular dihydrofolate reductase (DHFR) activity in HepG2 cells after 24, 48 and 72 h of incubation.

Treatment	Dihydrofolate reductase (DHFR) activity		
	24 h	48 h	72 h
Sham control	27.3±2.2	26.1±2.3	27.5±2.3
Methotrexate control	11.3±0.9[b]	9.1±0.7[b]	5.7±0.4[b]
Ursolic acid	28.1±2.3	25.4±2.0	23.1±2.0[a]
Derivative UA-1	23.2±1.9	21.3±1.7[a]	19.6±1.6[b]
Derivative UA-2	17.5±1.3[b]	13.7±1.2[b]	9.4±1.1[b]
Derivative UA-3	24.6±0.8	21.5±2.1[a]	17.5±1.4[b]

DHFR activity is expressed as IU/10^6 cells. All values are mean±standard error of samples (in triplicate) from four different experiments in each group. ([a]$p<0.05$, [b]$p<0.01$: indicate significance of difference between ursolic acid or its derivatives treatment and control treatment groups.)

C-28 position of UA [37]. In the current report, we tested whether UA derivatization can modulate one-carbon metabolism in HepG2 cells. We found that this triterpene can indeed mediate DHFR inhibition-induced cytotoxicity through down-regulation of one-carbon metabolism.

The mechanism by which *O. sanctum* extracts exhibit anti-cancer activity is complex and not fully understood as yet, especially regarding effect on one-carbon metabolism. Since DHFR has a key role in DNA synthesis of rapidly dividing cells, it could be one of the enzymes influenced by UA and its derivatives. Present results indicated time dependent decrease in DHFR activity after incubation with UA-1, UA-2 and UA-3. Significant decline in DHFR might decrease flux of folate pool for thymidylate synthesis, which in turn may compromise cell proliferation. Overall, these studies demonstrated most significant inhibition of DHFR activity when HepG2 cells were treated with UA-2 derivative. Reduced availability of thymidylate due to DHFR inhibition might therefore become rate limiting for DNA synthesis in cell exposed to UA derivatives [38]. It is therefore clear that attenuation of DHFR activity in response to inhibitory effect of UA and its derivative UA-2 might be detrimental for cellular functions of cancer cells. Thus far, perturbations of DHFR after exposure to UA and its derivatives have not been described in detail. Present studies, for the first time indicated that derivatives of UA might significantly reduce DHFR enzyme in cancer cells and might significantly contribute to the anti-neoplastic effects in cancer chemotherapy. Inhibition of DHFR activity and enhanced levels of extracellular Hcy may adversely affect nucleotide synthesis, which may further lead to cancer cell death [39, 40]. Earlier studies have shown that cancer cells exhibit increased intrinsic reactive oxygen species (ROS) stress, due to increased metabolic activity and mitochondrial malfunction [41]. Synergistic interaction of radiation-generated ROS with UA has also been shown. Therefore mechanistic basis for observed effect of UA and its derivatives on cancer cells might involve amplification of ROS stress in cancer cells [42]. Such results emphasize the complexity of how a cell may regulate crucial biosynthetic steps by regulating concentration of crucial enzymes. In brief, present data clearly showed down-regulation of HepG2 cells DHFR activity in response to UA derivatives in general and UA-2 in particular. The above results indicate that *O. sanctum* extract can serve as a useful source of bioactive compounds, such as UA, which can be modified to more potent bioactive derivatives [43].

Despite the side effects of chemotherapy and radiation therapy, there is no phytochemical that is effective and approved for patient care. In this context, present studies propose UA and particularly its derivative UA-2 as agent with significant anti-cancer effects. Measurement of DHFR and extracellular Hcy indicated impaired one-carbon metabolism and significant anti-proliferation effect in cancer cells treated with UA derivatives. Present studies also demonstrated that ester functionality at C-3 is essential for the pharmacological activities of pentacyclic triterpenes, and a hydrogen donor group at either C-3 position and/or C-28 position of UA is essential for the cytotoxic activity. However present data is still a very preliminary step, further studies, specifically clinical studies, are needed.

Acknowledgments: The authors wish to thank Dr. Gadge, Principal, Sterling College of Pharmacy for his guidance and support in carrying out this work. The authors gratefully acknowledge the assistance of Mr. Hanumant in conducting the experiments. The authors also wish to thank Mr. Shyam for his expert technical assistance.

Conflict of interest statement: The authors report no conflict of interest. The authors alone are responsible for the content and writing of the paper.

Received June 11, 2013; accepted August 5, 2013; previously published online September 7, 2013

References

1. Magesh V, Lee JC, Ahn KS, Lee HJ, Lee HJ, Lee EO, et al. Ocimum sanctum induces apoptosis in A549 lung cancer cells and suppresses the in vivo growth of Lewis lung carcinoma cells. Phytother Res 2009;23:1385–91.
2. Khanna A, Shukla P, Tabassum S. Role of *Ocimum sanctum* as a genoprotective agent on chlorpyrifos-induced genotoxicity. Toxicol Int 2011;18:9–13.
3. Ali M. Indigenous traditional drugs. In: Textbook of pharmacognosy. 1st ed. Delhi: CBS Publishers and Distributors, 1994:312–3. ISBN: 9788123902784.
4. Gupta P, Yadav DK, Siripurapu KB, Palit G, Rakesh M. Constituents of Ocimum sanctum with antistress activity. J Nat Prod 2007;70:1410–6.
5. Kim SC, Magesh V, Jeong SJ, Lee HJ, Ahn KS, Lee HJ, et al. Ethanol extract of Ocimum sanctum exerts anti-metastatic activity through inactivation of matrix metalloproteinase-9 and enhancement of anti-oxidant enzymes. Food Chem Toxicol 2010;48:1478–82.
6. Geetha RK, Kedlaya R, Vasudevan DM. Inhibition of lipid peroxidation by botanical extracts of Ocimum

sanctum: in vivo and in vitro studies. Life Sci 2004; 76:21–8.
7. Dahiya K, Sethi J, Dhankhar R, Singh V, Singh SB, Yadav M, et al. Effect of Ocimum sanctum on homocysteine levels and lipid profile in healthy rabbits. Arch Physiol Biochem 2011;117:8–11.
8. Anandjiwala S, Kalola J, Rajani M. Quantification of eugenol, luteolin, ursolic acid, and oleanolic acid in black (krishna tulasi) and green (sri tulasi) varieties of Ocimum sanctum Linn. Using high-performance thin-layer chromatography. J AOAC Int 2006;89:1467–74.
9. Harmand PO, Duval R, Liagre B, Jayat-Vignoles C, Beneutout JL, Delage C, et al. Ursolic acid induces apoptosis through caspase-3 activation and cell cycle arrest in HaCat cells. Int J Oncol 2003;23:105–12.
10. Ren D, Zuo R, González Barrios A, Bedzyk LA, Eldridge GR, Pasmore ME, et al. Differential gene expression for investigation of Escherichia coli biofilm inhibition by plant extract ursolic acid. Appl Environ Microbiol 2005;71:4022–34.
11. Baricevic D, Sosa S, Della Loggia R, Tubaro A, Simonovska B, Zupancic A, et al. Topical anti-inflammatory activity of Salvia officinalis L. leaves: the relevance of ursolic acid. J Ethnopharmcol 2001;75:125–32.
12. Rhu SY, Oak MH, Yoon SK, Cho DI, Yoo G-S, Kim TS, et al. Anti-allergic and anti-inflammatory triterpenes from the herb of Prunella vulgaris. Planta Med 2000;66:358–60.
13. Yim EK, Lee MJ, Lee KH, Um SJ, Park JS. Antiproliferative and antiviral mechanisms of ursolic acid and dexamethasone in cervical carcinoma cell lines. Int J Gynecol Cancer 2006;16:2023–31.
14. Robert HC, Samir AK. Chemistry, biological activity, and chemotherapeutic potential of betulinic acid for the prevention and treatment of cancer and HIV infection. Med Res Reviews 2004;24:90–114.
15. Huige L, Ulrich F. Prevention of atherosclerosis by interference with the vascular nitric oxide system. Curr Pharma Design 2009;15:3133–45.
16. Ifeanyi JA. Facilitating understanding of the purine nucleotide cycle and the one-carbon pool: part II: metabolism of the one-carbon pool. Biochem Mol Biol Educat 2005;33:255–9.
17. Ebere CA, Ijeoma K. Biochemical impedance on intracellular functions of vitamin B12 in chronic toxigenic mold exposures. Sci World J 2007;7:1649–57.
18. Abalo C, Afif AN, Souad B, Damien E, Pauline MA, Jean LG. Time course gene expression in the one-carbon metabolism network using HepG2 cell line grown in folate-deficient medium. J Nutr Biochem 2009;20:312–20.
19. Narasimha KR, Venkatachalam SR. Inhibition of dihydrofolate reductase and cell growth activity by the phenanthroin-dolizidine alkaloids pergularinine and tylophorinidine: the in vitro cytotoxicity of these plant alkaloids and their potential as antimicrobial and anticancer agents. Toxicol In Vitro 2000;14:53–9.
20. Stuart RS, John FM. Kinetic mechanism of the reaction catalyzed by dihydrofolate reductase from Escherichia coli. Biochem 1982;21:3757–65.
21. John FM, Stuart RS. Mechanism of the reaction catalyzed by dihydrofolate reductase from Escherichia coli: pH and deuterium isotope effects with NADPH as the variable substrate. Biochemistry 1988;27:5499–506.
22. Alexis N, Steve AW, Kevin M, Paul FG, John EH. Comparative folate metabolism in humans and malaria parasites (part I): pointers for malaria treatment from cancer chemotherapy. Trends Parasitol 2005;21:292–8.
23. Oae S, Kitao T, Kawamura S. Model pathways for enzymatic oxidative demethylation—II: polonovski reaction of N, N-dimethylaniline N-oxide, pummerer reactions of dimethyl, n-butyl methyl and methionine sulphoxide with acetylating agents and their implications in enzymatic demethylation. Tetrahedron 1963;19:1783–8.
24. Fernanda GS, Mayra DB, Sergio T, José NN, Vania D. Acute stressor-selective effects on homocysteine metabolism and oxidative stress parameters in female rats. Pharmacol Biochem Behavior 2006;85:400–7.
25. Chao MM, Shao QC, Jing RC, Rui QW, Peng FT, Masao H, et al. The cytotoxic activity of ursolic acid derivatives. Eur J Med Chem 2005;40:582–9.
26. Yanqiu M, Yanling S, Zhaokai Y, Yan X. Synthesis and invitro cytoxicity of novel ursolic acid derivatives. Molecules 2010;15:4033–40.
27. Friedkin M, Crawford EJ, Humphreys S, Goldin A. Inhibition of thymidylate synthetase and dihydrofolate reductase by naturally occurring oligoglutamate derivatives of folic acid. J Biol Chem 1975;250:5614–21.
28. Michael AH. Self-medicative behavior in the African great apes: an evolutionary perspective into the origins of human traditional medicine. BioScience 2001;51:651–61.
29. Ichikawa H, Nakamura Y, Kashiwada Y, Aggarwal BB. Anticancer drugs designed by mother nature: ancient drugs but modern targets. Curr Pharm Design 2007;13:3400–16.
30. Alan H. Strategies for discovering drugs from previously unexplored natural products. Drug Disc Today 2000;5:294–300.
31. Efferth T, Koch E. Complex interactions between phytochemicals. The multi-target therapeutic concept of phytotherapy. Curr Drug Targets 2011;12:122–32.
32. Richard BB, Natasa P. Multitargeted therapy of cancer by lycopene. Cancer Lett 2008;269:339–51.
33. Balanehru S, Nagarajan B. Protective effect of oleanolic acid and ursolic acid against lipid peroxidation. Biochem Int 1991;24:981–90.
34. Manu KA, Girija K. Ursolic acid induces apoptosis by activating p53 and caspase-3 gene expressions and suppressing NF-κB mediated activation of bcl-2 in B16F-10 melanoma cells. Int Immunopharmacol 2008;8:974–81.
35. Shyu MH, Kao TC, Yen GC. Oleanolic acid and ursolic acid induce apoptosis in HuH7 human hepatocellular carcinoma cells through a mitochondrial-dependent pathway and downregulation of XIAP. J Agric Food Chem 2010;58:6110–8.
36. Sahdeo P, Vivek RY, Ramaswamy K, Bharat BA. Ursolic acid, a pentacyclin triterpene, potentiates TRAIL-induced apoptosis through p53-independent up-regulation of death receptors. J Biol Chem 2011;286:5546–57.
37. Kashiwada Y, Chiyo J, Ikeshiro Y, Nagao T, Okabe H, Cosentino LM, et al. Synthesis and anti-HIV activity of 3-alkylamido-3-deoxy-betulinic acid derivatives. Chem Pharm Bull 2000;48:1387–90.
38. Hu CM, Yeh MT, Tsao N, Chen CW, Gao QZ, Chang CY, et al. Tumor cells require thymidylate kinase to prevent dUTP incorporation during DNA Repair. Cancer Cell 2012;22:36–50.

39. Mark PM, Inna IK, Wenzhen D. Folic acid and homocysteine in age-related disease. Ageing Res Rev 2002;1:95–111.
40. Blume SW, Snyder RC, Ray R, Thomas S, Koller CA, Miller DM. Mithramycin inhibits SP1 binding and selectively inhibits transcriptional activity of the dihydrofolate reductase gene in vitro and in vivo. J Clin Invest 1991;88:1613–21.
41. Pelicano H, Carney D, Huang P. ROS stress in cancer cells and therapeutic implications. Drug Resist Updat 2004;7:97–110.
42. Koh SJ, Tak JK, Kim ST, Nam WS, Kim SY, Park KM, et al. Sensitization of ionizing radiation-induced apoptosis by ursolic acid. Free Radic Res 2012;46:339–45.
43. Gayathri C, Indira J, Alan M, Tom S, Stephen S. Structure-dependent inhibition of bladder and pancreatic cancer cell growth by 2-substituted glycyrrhetinic and ursolic acid derivatives. Bioorg Med Chem Lett 2008;18: 2633–9.